

# Dynamic response of a single-electron transistor in the ac Kondo regime

Thanh Thi Kim Nguyen

*Department of Physics, University of Cincinnati, Cincinnati, Ohio 45221, USA*

(Dated: July 1, 2021)

A single-electron transistor (SET) in a magnetic field irradiated with microwaves is studied theoretically in non-equilibrium Kondo regime. The two fold effect of frequency- $\Omega$ -microwaves is considered as follows: the oscillations in the voltage with frequency  $\Omega$  and in the coupling parameters with frequency  $\Omega/p$  ( $p \in \mathbb{N}$ ). We describe the system by the Kondo model at a specific point in the Toulouse limit. A non-perturbative technique is proposed, namely, the non-equilibrium Green's functions and physical observables are averaged over a period of  $2\pi p/\Omega$ . When the microwave irradiation is considered affecting only the voltage, one sees the Kondo satellites as stated in the previous studies. Moreover, the features of the differential conductance and magnetic susceptibility of a SET become richer when the Kondo couplings are considered oscillating on time. We obtain the satellite peak splitting. It explains the possibilities one can find in experimental results that the distance between peaks, which appear in the differential conductance – magnetic amplitude characteristics  $G(H)$  or in the differential conductance – dc voltage characteristics  $G(V_{dc})$ , can be smaller than  $\hbar\Omega$ .

PACS numbers: 72.10.Fk, 72.15.Qm, 73.40.Gk

## I. INTRODUCTION

The Kondo effect, stemming from a macroscopic quantum coherent coupling between a localized magnetic moment and a Fermi sea of electrons, has been used to explain successfully many extraordinary properties of bulk dilute magnetic alloy systems [1, 2] for a long time. Based on the developments in mesoscopic physics and nanotechnology, it has been proposed to study the systems of reduced dimensions and the single impurity problems. The latter is also represented by the very rapidly developing fields of quantum dots (QDs), where Kondo-like impurities are manufactured [3–5]. The local magnetic moment is screened by hybridization with the delocalized electron-spins, leading to the formation of a bound spin-singlet state. A many-body resonance in the density of states (DOS) appears at the Fermi energy, which strongly influences the conductance of the system at low temperatures. Above the Kondo temperature, thermal fluctuations destroy the coherence, resulting in a non-monotonic dependence of the conductance on temperature. Under the Kondo temperature, due to the Kondo correlations, the system becomes dynamic and can be controlled experimentally by tuning external parameters such as source-drain voltage, gate voltage, and magnetic field [4].

Since the Kondo effect is a typical example of a strongly correlated system, it is of particular interest in the field of non-equilibrium phenomena [6, 7]. As our understanding of the Kondo effect for a time-independent bias has increased [6, 7], the theoretical effort has turned to time-varying fields [8–14]. The ac field produces satellite peaks in the dependence of the differential conductance on the dc bias, as a consequence of the fact that the microwave field gives rise to effective changes in the DOS versus energy which are dramatically illustrated in the tunnel-

ing current [15]. However, this interesting result could not be observed experimentally until 2004 by Kastner's group [16]. They measured the differential conductance of a SET irradiated with high frequency microwaves. The results show that when the photon energy is somewhat greater than the Kondo temperature and the microwave voltage is carefully chosen, single-photon satellite peaks in the differential conductance can be observed. Very recently, Kogan's group has investigated the differential conductance as a function of magnetic field for different high frequencies of microwaves [17]. The non-trivial dynamics that emerges when external parameters compete with the Kondo correlations has attracted our attention to study the Kondo effect in a SET irradiated with microwaves. Due to the complexity of out-of-equilibrium many-body systems, it is instructive to investigate those cases where the exact non-perturbative solutions are accessible. One particular interesting case is the Kondo model in the Toulouse limit, which has been solved exactly in equilibrium [18] as well as out of equilibrium (SH theory) [10]. A question arising from the SH theory [10], which is related to the experiment, is what happens if the Kondo coupling parameters are also affected by microwave irradiation. We can have different scenarios in different experiments: i, only the voltage oscillates; ii, only the Kondo couplings oscillate; iii, both of them oscillate [19]. Moreover, the multi-effect of microwave irradiation can induce the fact that the voltage oscillates with frequency  $\Omega$ , the Kondo couplings oscillate with frequency  $\Omega_1 = \Omega/p$ ,  $p \in \mathbb{N}$  in an appropriate experimental set-up. We predict that  $p$  is a frequency-dependent systematic parameter.

In this paper we investigate the response of a SET to a simultaneous application of a magnetic field and a high frequency microwave irradiation. We consider Kondo couplings oscillating with a frequency integer

times smaller than the frequency of microwaves. We solve the problem non-perturbatively by averaging non-equilibrium Green's functions in the period of the slow oscillation. The differential conductance and the magnetic susceptibility are computed. In these results, the Kondo satellites appear due to the oscillation of the source-drain voltage. These satellites are split when the oscillation of Kondo couplings is taken into account. The peak splitting distance depends on the difference between the input frequency and the frequency of the Kondo couplings, which is assumed to be a natural number  $p$ .

This paper is organized as follows. In section II, the time-dependent Kondo model in the Toulouse limit with time dependent Kondo couplings  $J_\lambda^{\alpha\beta}(t)$  is introduced and mapped onto a quadratic effective Hamiltonian. The averaged non-equilibrium Green's function method used to calculate the differential conductance and the magnetic susceptibility is presented in section III. The results for the differential conductance and the magnetic susceptibility are presented in section IV. We conclude our results in section V.

## II. TIME DEPENDENT KONDO MODEL

### A. Model and proposal for time-dependent Kondo couplings

The system we study is a QD attached to two leads by high resistance junctions, so that the charge of the dot is quantized. The Kondo effect emerges in a QD occupied by an odd number of electrons at temperatures below the mean level spacing in the dot. Under such conditions, the system can be described by a single-impurity Anderson model with the level spacing playing the role of cutoff in it [20]. Moreover, we consider the dot in the Kondo regime: both ionization and electron addition energy are much bigger than the tunneling rates:  $\{E_d, U - E_d\} \gg \Gamma_{L/R}$ , and the applied fields do not drive the dot out of this regime:  $\{eV_{dc}, eV_{dot}, eV_{ac}, \mu_B g_i B\} < \{E_d, U - E_d\}$ . Hence, the Anderson model can be mapped onto a two lead Kondo model through a time dependent Schrieffer-Wolff transformation [11, 13].

In our proposed Kondo model, the two non-interacting leads of spin-1/2 electrons, labeled right (R) and left (L), each subjects to a separate time-dependent voltage, interact via an exchange coupling with a spin-1/2 impurity moment  $\vec{\tau}$  placed in between them. The conduction electrons in each lead, that couple to the impurity, are described by one dimensional fields  $\psi_{\alpha\sigma}^\dagger(x)$ , where  $\alpha = L, R$ , and  $\sigma = \uparrow, \downarrow$  are lead and spin indices, respectively. The interaction  $\vec{J}^{\alpha\beta}$  of conduction electrons in the leads and the impurity is local in space at  $x = 0$  and involves the conduction-electron spin densities, which are written as  $(\vec{s})_{\alpha,\beta} = \frac{1}{2} \sum_{\sigma,\sigma'} \psi_{\alpha\sigma}^\dagger(0) (\vec{\sigma})_{\sigma,\sigma'} \psi_{\beta\sigma'}(0)$ .

Thus, the time-dependent Kondo Hamiltonian describing a SET in a magnetic field and irradiated with microwaves is

$$\begin{aligned} \mathcal{H} = & iv_F \sum_{\alpha=L,R;\sigma=\uparrow,\downarrow} \int_{-\infty}^{\infty} dx \psi_{\alpha\sigma}^\dagger \frac{\partial}{\partial x} \psi_{\alpha\sigma} \\ & + \frac{V(t)}{2} \sum_{\sigma=\uparrow,\downarrow} \int_{-\infty}^{\infty} dx \left[ \psi_{L\sigma}^\dagger \psi_{L\sigma} - \psi_{R\sigma}^\dagger \psi_{R\sigma} \right] \\ & + \sum_{\alpha,\beta=L,R} \sum_{\lambda=x,y,z} J_\lambda^{\alpha\beta}(t) s_{\alpha\beta}^\lambda \tau^\lambda - H\tau^z. \end{aligned} \quad (1)$$

The system is driven out of equilibrium by applying a voltage bias across the junction,  $V(t) = V_{dc} + V_{ac} \cos(\Omega t)$ . The dc part  $V_{dc}$  fixes a chemical-potential difference between the two Fermi seas. The ac part  $V_{ac} \cos(\Omega t)$  fluctuates these two chemical-potentials as an oscillation on time, allowing us to average the Green's functions, which will be shown in detail in the next section. We notice that we adopt atomic units with  $\hbar = k_B = e = \mu_B g_i = 1$  in this paper.

In general, due to the microwave irradiation, the couplings are split into two parts: the time-independent part and the time-dependent part, which oscillates on time, as

$$J_\lambda^{\alpha\beta}(t) = J_{\lambda 0}^{\alpha\beta} + J_{\lambda 1}^{\alpha\beta} \cos(\Omega_1 t + \phi_{\alpha\beta}), \quad (2)$$

$\alpha, \beta = L, R$  imply the left and right leads. The oscillation frequency  $\Omega_1$  of couplings is different from the microwave frequency  $\Omega$ . In order to enter the exact solvable situation, we assume [10, 18, 21]

$$J_z^{LR} = J_z^{RL} = 0, \quad J_z^{LL} = J_z^{RR} = J_z = 2\pi v_F. \quad (3)$$

If the SET is in equilibrium or if a dc voltage is applied, the coupling parameters are constant and equal to  $J_{\perp 0}^{\alpha\beta}$ . In equilibrium case, from the scaling equations to lowest order in the couplings, we find that the constraints in equation (3) remain stable upon scaling if either

$$J_{\perp 0}^{LL} = J_{\perp 0}^{RR}, \quad J_{\perp 0}^{RL} = 0, \quad (4)$$

or

$$J_{\perp 0}^{LL} = -J_{\perp 0}^{RR}. \quad (5)$$

As stated in Ref. [21], these two cases correspond to two distinct isotropic two-channel Kondo model. We notice that in the constraint (4), the two leads are decoupled, the channels are just the right and left leads, which carry no current. When the system is irradiated with microwaves, both the voltage bias and the perpendicular couplings are proposed oscillating on time. The model in this paper is anisotropic in real space. It cannot be obtained by the direct mapping from the Anderson model to the Kondo model. However, the experimentalists can apply the relations between the Kondo couplings and the

tunneling rates, which are stated in Refs. [11, 13], in order to compare their experimental results to the results in our theory.

For simplicity, we propose the time dependent perpendicular coupling parameters as

$$\begin{aligned} J_{\perp}^{RL}(t) &= J_{\perp}^{LR}(t) = J_{\perp}^{RL} \cos(\Omega_1 t) , \\ J_{\perp}^{LL}(t) &= J_{\perp 0}^{LL} + J_{\perp}^{LL} \cos(\Omega_1 t) , \\ J_{\perp}^{RR}(t) &= J_{\perp 0}^{RR} + J_{\perp}^{RR} \cos(\Omega_1 t) . \end{aligned} \quad (6)$$

This proposal can be justified qualitatively as follows. The oscillation of  $J(t)$  comes from the oscillations of voltages such as source-drain voltage and gate voltage. The voltage biases oscillate with the same frequency  $\Omega$ , as the frequency of microwaves. The Kondo couplings thus oscillate with frequency  $\Omega$ . However, experimentalists can think about some experimental set-ups, in which one can control the frequencies of different voltages or the phases between voltage biases oscillate on time. The goal of this work is to have the Kondo couplings  $J(t)$  oscillating on time with frequency  $\Omega_1 \neq \Omega$ . For simplicity, we assume either  $\Omega_1 = p\Omega$  or  $\Omega_1 = \Omega/p$ ,  $p \in \mathbb{N}$ . Since the  $\Omega_1 = \Omega/p$  assumption is predicted to give the results of satellite splitting, it is chosen to be studied first. The  $\Omega_1 = p\Omega$  assumption will be represented later.

Besides, one can investigate the time dependence of Kondo couplings in a general form as shown in equation (2). However, the goal of this paper is to investigate the effects of the microwave irradiation. We thus consider the Kondo couplings as shown in equations (6). Since we consider the time average of observables, we can neglect the phase difference among the coupling parameters. In general, microwave irradiation changes the transverse couplings  $J_{\perp}^{RL}(t)$ , thus changes the channel isotropy. We find that a QD either in a magnetic field [22], or irradiated with microwaves can be driven out of the isotropic two channel Kondo limit.

## B. Mapping onto a solvable model

The procedure to arrive at a solvable model is given in the following. We first bosonize the Hamiltonian (1) with notice that we have considered Klein factors and assumed the length was infinity:

$$\psi_{\alpha\sigma}(x) = \frac{F_{\alpha\sigma}}{\sqrt{2\pi a}} e^{-i\Phi_{\alpha\sigma}(x)} , \quad (7)$$

where  $\Phi_{\alpha\sigma}(x) = \sqrt{\pi} \left[ \int_{-\infty}^x dx' \Pi_{\alpha\sigma}(x') - \phi_{\alpha\sigma}(x) \right]$ . Here  $\phi_{\alpha\sigma}(x)$  are Bose fields and  $\Pi_{\alpha\sigma}(x)$  are their conjugate momenta, satisfying commutation relations [23]. The next step is introducing new bosonic fields: charge  $\phi_c(x)$ , pseudo-spin  $\phi_s(x)$ , flavor  $\phi_f(x)$ , and pseudo-flavor  $\phi_{sf}(x)$  as  $\phi_c(x) = \left( \sum_{\alpha,\sigma} \phi_{\alpha\sigma} \right) / 2$ ,  $\phi_s(x) =$

$\left( \sum_{\alpha,\sigma} \sigma_{\alpha\sigma}^z \phi_{\alpha\sigma} \right) / 2$ ,  $\phi_f(x) = \left( \sum_{\alpha,\sigma} \sigma_{\alpha\sigma}^z \phi_{\alpha\sigma} \right) / 2$ ,  $\phi_{sf}(x) = \left( \sum_{\alpha,\sigma} \sigma_{\alpha\sigma}^z \sigma_{\sigma\sigma}^z \phi_{\alpha\sigma} \right) / 2$ , and also for  $\Pi_{\nu}$ ,  $\Phi_{\nu}$ ,  $N_{\nu}$ ,  $\nu = c, s, f, sf$ . We then perform the transformation of the Hamiltonian  $\mathcal{U}\mathcal{H}\mathcal{U}^{-1}$  with  $\mathcal{U} = \exp[-i\tau^z \Phi_s(0)]$ . Four more Klein factors  $F_{\nu}$  are introduced, which satisfy  $[F_{\nu}, N_{\nu'}] = \delta_{\nu\nu'} F_{\nu}$  and relate to the old ones as  $F_{L\downarrow}^{\dagger} F_{L\uparrow} = F_s F_{sf}$ ,  $F_{R\downarrow}^{\dagger} F_{R\uparrow} = F_s F_{sf}^{\dagger}$ ,  $F_{R\downarrow}^{\dagger} F_{L\uparrow} = F_f F_s$ ,  $F_{R\uparrow}^{\dagger} F_{L\downarrow} = F_f F_s^{\dagger}$ . The new impurity fermion is thus represented as  $d^{\dagger} = F_s \tau^+$ ,  $d = F_s^{\dagger} \tau^-$ ,  $\tau^z = d^{\dagger} d - 1/2$ . We now re-fermionize these bosonic fields as

$$\Psi_m(x) = \frac{1}{\sqrt{2\pi a}} F_m e^{-i\Phi_m(x)} \quad (8)$$

to re-write the Hamiltonian in which all the charge, spin, flavor, and spin flavor degrees of freedom are separated

$$\begin{aligned} \mathcal{H}' &= iv_F \sum_{\nu=c,s,f,sf} \int_{-\infty}^{\infty} dx \psi_{\nu}^{\dagger}(x) \partial_x \psi_{\nu}(x) \\ &+ [H - (J_z - 2\pi v_F) : \psi_s^{\dagger}(0) \psi_s(0) :] (d^{\dagger} d - 1/2) \\ &+ \int_{-\infty}^{\infty} dx [V_{dc} + V_{ac} \cos(\Omega t)] \psi_f^{\dagger}(x) \psi_f(x) \\ &+ \frac{J_t(t)}{2\sqrt{2\pi a}} [\Psi_f^{\dagger}(0) - \Psi_f(0)] (d + d^{\dagger}) \\ &+ \frac{J_a(t)}{2\sqrt{2\pi a}} [\Psi_{sf}^{\dagger}(0) - \Psi_{sf}(0)] (d + d^{\dagger}) \\ &+ \frac{J_s(t)}{2\sqrt{2\pi a}} [\Psi_{sf}^{\dagger}(0) + \Psi_{sf}(0)] (d^{\dagger} - d) , \end{aligned} \quad (9)$$

where  $:\psi_s^{\dagger}(0)\psi_s(0):$  means normal ordering with respect to the unperturbed  $\psi_s$  Fermi sea, and we have defined  $J_t(t) = J_{\perp}^{LR}(t) = J_{\perp}^{RL} \cos(\Omega_1 t)$ ,  $J_s(t) = (J_{\perp 0}^{LL} + J_{\perp 0}^{RR}) / 2 + (J_{\perp}^{LL} + J_{\perp}^{RR}) \cos(\Omega_1 t) / 2$ ,  $J_a(t) = (J_{\perp}^{LL} - J_{\perp}^{RR}) \cos(\Omega_1 t) / 2$ . From our assumption in equation (3),  $J_z = 2\pi v_F$ , we are in the Emery-Kivelson line [18], the Hamiltonian (9) reduces to quadratic form, which is exactly solvable in equilibrium [18] and in the SH theory [10, 21]. The charge and spin sectors are decoupled from the local flavor and spin flavor, reduced to a collection of uncoupled harmonic oscillators. Therefore, they will be omitted from now on. Finally, by introducing Majorana fermions  $\hat{a} = (d^{\dagger} + d) / \sqrt{2}$  and  $\hat{b} = (d^{\dagger} - d) / i\sqrt{2}$ , one arrives at the following Hamiltonian

$$\begin{aligned} \mathcal{H} &= \sum_k \left[ \varepsilon_{fk}(t) c_{fk}^{\dagger} c_{fk} + \varepsilon_{sfk} c_{sfk}^{\dagger} c_{sfk} \right. \\ &- iH\hat{a}\hat{b} + \frac{J_t(t)}{2\sqrt{\pi a}} (c_{fk}^{\dagger} - c_{fk}) \hat{a} \\ &\left. + \frac{iJ_s(t)}{2\sqrt{\pi a}} (c_{sfk}^{\dagger} + c_{sfk}) \hat{b} + \frac{J_a(t)}{2\sqrt{\pi a}} (c_{sfk}^{\dagger} - c_{sfk}) \hat{a} \right] , \end{aligned} \quad (10)$$

where  $\varepsilon_{fk}(t) = 2\pi v_F k + e[V_{dc} + V_{ac} \cos(\Omega t)]$ ,  $\varepsilon_{sfk} = 2\pi v_F k$ . Here after we will work with Hamiltonian (10) to calculate physical observables.

### III. AVERAGE GREEN'S FUNCTIONS

The Keldysh Green's function technique is well known as an efficient method to solve non-equilibrium problems [24]. This technique has been applied to express the fully nonlinear, time dependent current through interacting and non-interacting resonant tunneling systems [25]. However, the complete result only obtained for the case level-width function (or tunneling amplitude) is time independent. Similarly, the Hamiltonian (10) with constant couplings has been solved exactly [10]. Later, the steady state in the Kondo model in the Toulouse limit, in which the couplings are periodically switched on and off, has been investigated by analyzing exact analytical results for the local spin dynamics at zero temperature [26]. The exact solution for the time dependent Hamiltonian (10) still remains. In this section, we present our average Keldysh non-equilibrium Green's function method which gives good results in the high frequency regime.

#### A. Non-interacting Green's functions of flavor fermions

Because the first effect of microwave irradiation induces the oscillation in the voltage bias as shown in the Hamiltonian (10), we first discuss the non-interacting Green's functions of the flavor fermion, which is defined as

$$g_{fk}(t, t') = -i \left\langle T_K \left\{ c_{fk}(t) c_{fk}^\dagger(t') \right\} \right\rangle. \quad (11)$$

The flavor fermion is considered as in the two dimensional fermion sea. The retarded, advanced, and Keldysh components are

$$\begin{aligned} g_{fk}^{R,A}(t, t') &= \mp i \Theta(\pm t \mp t') e^{-i2\pi v_F k(t-t')} \\ &\quad \times e^{-i\frac{V_{ac}}{\Omega} [\sin(\Omega t) - \sin(\Omega t')]}, \\ g_{fk}^K(t, t') &= i [2f(2\pi v_F k + V_{dc}) - 1] e^{-i2\pi v_F k(t-t')} \\ &\quad \times e^{-i\frac{V_{ac}}{\Omega} [\sin(\Omega t) - \sin(\Omega t')]}, \end{aligned} \quad (12)$$

where  $f$  is the Fermi distribution function in the flavor lead. While the chemical potential of the spin flavor lead is chosen as the reference, the chemical potential of the flavor lead oscillates on time with an amplitude  $V_{ac}$  around the fixed chemical potential  $V_{dc}$ . Using the identity  $\exp[x(a-1/a)/2] = \sum_{n=-\infty}^{\infty} a^n J_n(x)$ , where  $J_n(x)$  are the integer Bessel functions of the first kind,

and changing variables

$$\begin{aligned} \tau &= t - t', \\ T &= \frac{t + t'}{2}, \end{aligned} \quad (13)$$

we find

$$\begin{aligned} g_{fk}^{R,A}(\tau, T) &= \mp i \Theta(\pm \tau) \sum_{m,n=-\infty}^{\infty} J_n\left(\frac{V_{ac}}{\Omega}\right) J_m\left(\frac{V_{ac}}{\Omega}\right) \\ &\quad \times e^{-i[\varepsilon_k + (n+m)\Omega/2]\tau} e^{-i\Omega(n-m)T}. \end{aligned} \quad (14)$$

Because the flavor fermion chemical potential oscillates on time with frequency  $\Omega$ , one can take the average of the non-interacting Green's function over time  $T \gg \Omega^{-1}$  [27]. The Fourier transform regarding the time difference  $\tau$  of the average Green's function is

$$\begin{aligned} \overline{g_f^{R,A}(\omega)} &= \sum_k \overline{g_{fk}^{R,A}(\omega)} \\ &= \sum_{m,n=-\infty}^{\infty} J_n^2\left(\frac{V_{ac}}{\Omega}\right) \sum_k \frac{1}{\omega - 2\pi v_F k - n\Omega}. \end{aligned} \quad (15)$$

The DOS of the flavor fermion is [15]

$$\begin{aligned} \overline{\rho_f(\omega)} &= \sum_n J_n^2\left(\frac{V_{ac}}{\Omega}\right) \rho(\omega - n\Omega) \\ &= \sum_n J_n^2\left(\frac{V_{ac}}{\Omega}\right) \frac{1}{2\pi v_F} = \frac{1}{2\pi v_F}. \end{aligned} \quad (16)$$

We have the second line because we have applied the linearization for the energy spectrum around the Fermi level [23]. The retarded and advanced components thus remain as those in equilibrium

$$\overline{g_f^{R,A}(\omega)} = \mp \frac{i}{2v_F}. \quad (17)$$

However, the effect of ac voltage  $V_{ac}(t)$  modifies the Keldysh component  $g_{fk}^K(t, t')$  as

$$\begin{aligned} \overline{g_f^K(\omega)} &= \sum_k \overline{g_{fk}^K(\omega)} \\ &= \frac{i}{v_F} \sum_n J_n^2\left(\frac{V_{ac}}{\Omega}\right) [2f(\omega - n\Omega + V_{dc}) - 1], \end{aligned} \quad (18)$$

with  $\overline{g_f^K(\omega)}$  is the average of the Keldysh component in the Fourier space corresponding the time difference  $\tau$ .

We then calculate the combined non-interacting Green's functions of the flavor fermion. We show here one example

$$m_{fk}(t, t') = -i \left\langle T_K \left[ c_{fk}^\dagger(t) + c_{fk}(t) \right] \left[ c_{fk}^\dagger(t') - c_{fk}(t') \right] \right\rangle. \quad (19)$$

Its retarded, advanced, and Keldysh components are  $\overline{m_f^{R,A}(\omega)} = 0$ ,

$$\begin{aligned} \overline{m_f^K(\omega)} &= (2i/v_F) \sum_n J_n^2 \left( \frac{V_{ac}}{\Omega} \right) \\ &\times \{f(\omega - n\Omega + V_{dc}) - f(\omega + n\Omega - V_{dc})\}. \end{aligned} \quad (20)$$

About the spin flavor fermion, its chemical potential is chosen as the reference, and no oscillation voltage is applied on the spin flavor lead, it is considered in equilibrium.

## B. Interacting Majorana Green's functions:

In order to compute observables, it is necessary to calculate advanced, retarded, and Keldysh components of Majorana Green's functions, which are defined as

$$G_{\alpha\beta}(t, t') = -i \langle T_K \{ \alpha(t) \beta(t') \} \rangle, \quad \alpha, \beta = \hat{a}, \hat{b}. \quad (21)$$

We show here the results of the Green's functions  $G_{aa}^A(t, t')$  and  $G_{ba}^K(t, t')$ , which are used to calculate the differential conductance and the magnetic susceptibility.

### 1. Advanced Green's function $G_{aa}^A(t, t')$ :

We write the Green's functions in terms of the interaction-picture operators by invoking the S matrix, we have the advance Green's functions as follows

$$\begin{aligned} G_{ba}^A(t, t') &= iH \int_{-\infty}^{\infty} dt_1 g_{bb}^A(t - t_1) G_{aa}^A(t_1, t') \\ &\quad + \frac{i}{4\pi av_F} \int_{-\infty}^{\infty} dt_1 J_s^2(t_1) g_{bb}^A(t - t_1) G_{ba}^A(t_1, t'), \\ G_{aa}^A(t, t') &= g_{aa}^A(t, t') - iH \int_{-\infty}^{\infty} dt_1 g_{aa}^A(t - t_1) G_{ba}^A(t_1, t') \\ &\quad + \frac{i}{4\pi av_F} \int_{-\infty}^{\infty} dt_1 [J_t^2(t_1) + J_a^2(t_1)] g_{aa}^A(t - t_1) G_{aa}^A(t_1, t'). \end{aligned} \quad (22)$$

With the assumption of coupling parameters  $J_i(t)$  from (10), we have

$$\begin{aligned} G_{ba}^A(t, t') &= -H \int_{-\infty}^{\infty} dt_1 \Theta(t_1 - t) G_{aa}^A(t_1, t') \\ &\quad - \int_{-\infty}^{\infty} dt_1 \Gamma_s(t_1) \Theta(t_1 - t) G_{ba}^A(t_1, t'), \\ G_{aa}^A(t, t') &= i\Theta(t' - t) + H \int_{-\infty}^{\infty} dt_1 \Theta(t_1 - t) G_{ba}^A(t_1, t') \\ &\quad - \int_{-\infty}^{\infty} dt_1 \Gamma_{at}(t_1) \Theta(t_1 - t) G_{aa}^A(t_1, t'), \end{aligned} \quad (23)$$

with

$$\begin{aligned} \Gamma_s(t) &= \Gamma_{s0} + 2\sqrt{\Gamma_{s0}\Gamma_s} \cos(\Omega_1 t) + \Gamma_s \cos^2(\Omega_1 t), \\ \Gamma_{at}(t) &= \Gamma_{at} \cos^2(\Omega_1 t), \end{aligned} \quad (24)$$

where we have defined  $\Gamma_t = (J_{\perp}^{RL})^2 / 4\pi av_F$ ,  $\Gamma_a = (J_{\perp}^{LL} - J_{\perp}^{RR})^2 / 16\pi av_F$ ,  $\Gamma_{at} = \Gamma_t + \Gamma_a$ ,  $\Gamma_{s0} = (J_{\perp 10}^{LL} + J_{\perp 10}^{RR})^2 / 16\pi av_F$ ,  $\Gamma_s = (J_{\perp}^{LL} + J_{\perp}^{RR})^2 / 16\pi av_F$ . Equations (23) induces the SH theory limit when all couplings are time independent. One can easily take Fourier transform of equations (23), then re-obtain the exact formulas of the advanced Majorana Green's functions, as shown in the formula (4.9) in Ref. [21].

We need to solve the integral equations (23) and find the Green's function  $G_{aa}^A(t, t')$ . We first change the equations (23) to differential equations by taking the derivative with respect to time  $t$ . We have

$$\begin{aligned} [\partial_t - \Gamma_s(t)] G_{ba}^A(t, t') &= H G_{aa}^A(t, t'), \\ [\partial_t - \Gamma_{at}(t)] G_{aa}^A(t, t') + H G_{ba}^A(t, t') &= -i\delta(t - t'). \end{aligned} \quad (25)$$

We define the non-interacting Green's functions  $g_{at/s}^A(t, t')$  as [28]

$$[\partial_t - \Gamma_{at/s}(t)] g_{at/s}^A(t, t') = \delta(t - t'), \quad (26)$$

so

$$\begin{aligned} g_{at}^A(t, t') &= -\Theta(t' - t) \exp\left[\frac{\Gamma_{at}}{2}(t - t')\right] \\ &\quad \times \exp\left[\frac{\Gamma_{at}}{4\Omega_1} [\sin(2\Omega_1 t) - \sin(2\Omega_1 t')]\right], \\ g_s^A(t, t') &= -\Theta(t' - t) \exp\left[\left(\Gamma_{s0} + \frac{\Gamma_s}{2}\right)(t - t')\right] \\ &\quad \times \exp\left[\frac{2\sqrt{\Gamma_{s0}\Gamma_s}}{\Omega_1} [\sin(\Omega_1 t) - \sin(\Omega_1 t')]\right] \\ &\quad \times \exp\left[\frac{\Gamma_s}{4\Omega_1} [\sin(2\Omega_1 t) - \sin(2\Omega_1 t')]\right] \end{aligned} \quad (27)$$

From equations (25) and (26), we have

$$\int_{-\infty}^{\infty} dt_1 \left[ [g_{at}^A(t, t_1)]^{-1} + H^2 g_s^A(t, t_1) \right] G_{aa}^A(t_1, t') = -i\delta(t - t'). \quad (28)$$

### 2. Keldysh Green's function $G_{ba}^K(t, t')$ :

In the same way as we did with the advanced Green's functions, we write the Keldysh Green's functions by invoking the S-matrix as

$$\begin{aligned} G_{ba}^K(t, t') &= \int_{-\infty}^{\infty} dt_1 H \Theta(t - t_1) G_{aa}^K(t_1, t') \\ &\quad - \int_{-\infty}^{\infty} dt_1 \Gamma_s(t_1) \Theta(t - t_1) G_{ba}^K(t_1, t') + H \Upsilon_s(t, t'), \end{aligned} \quad (29)$$



$$G_{aa}^K(t, t') = - \int_{-\infty}^{\infty} dt_1 H \Theta(t - t_1) G_{ba}^K(t_1, t') - \int_{-\infty}^{\infty} dt_1 \Gamma_{at}(t_1) \Theta(t - t_1) G_{aa}^K(t_1, t') + \Upsilon_{at}(t, t'), \quad (30)$$

where we have defined the  $\Upsilon_{at}(t, t')$ ,  $\Upsilon_s(t, t')$  as

$$\begin{aligned} \Upsilon_s(t, t') &= \int_{-\infty}^{\infty} dt_1 dt_2 \frac{J_s(t_1) J_s(t_2)}{4\pi^2 av_F} \Theta(t - t_1) \int_{-\infty}^{\infty} d\omega \\ &\times [2f(\omega) - 1] e^{-i\omega(t_1 - t_2)} \int_{-\infty}^{\infty} dt_3 g_s^A(t_2, t_3) G_{aa}^A(t_3, t'), \quad (31) \end{aligned}$$

$$\begin{aligned} \Upsilon_{at}(t, t') &= \int_{-\infty}^{\infty} dt_1 dt_2 \frac{J_t(t_1) J_t(t_2)}{4\pi^2 av_F} \Theta(t - t_1) \\ &\times \int_{-\infty}^{\infty} d\omega \sum_n J_n^2 \left( \frac{V_{ac}}{\Omega} \right) e^{-i\omega(t_1 - t_2)} G_{aa}^A(t_2, t') \\ &\times [f(\omega - n\Omega + V_{dc}) + f(\omega + n\Omega - V_{dc}) - 1] \\ &+ \int_{-\infty}^{\infty} dt_1 dt_2 \frac{J_a(t_1) J_a(t_2)}{4\pi^2 av_F} \Theta(t - t_1) \\ &\times \int_{-\infty}^{\infty} d\omega [2f(\omega) - 1] e^{-i\omega(t_1 - t_2)} G_{aa}^A(t_2, t'). \quad (32) \end{aligned}$$

The above equations induce the following differential equations

$$\begin{aligned} [\partial_t + \Gamma_s(t)] G_{ba}^K(t, t') &= H G_{aa}^K(t, t') + H \Lambda_s(t, t'), \\ [\partial_t + \Gamma_{at}(t)] G_{aa}^K(t, t') + H G_{ba}^K(t, t') &= \Lambda_{at}(t, t'), \quad (33) \end{aligned}$$

with  $\Lambda_{at/s}(t, t') = \partial_t \Upsilon_{at/s}(t, t')$ . We define non-interacting Green's functions  $g_{at/s}^K(t, t')$  as

$$[\partial_t + \Gamma_{at/s}(t)] g_{at/s}^K(t, t') = \delta(t - t'), \quad (34)$$

so

$$\begin{aligned} g_{at}^K(t, t') &= \Theta(t - t') \exp \left[ -\frac{\Gamma_{at}}{2} (t - t') \right] \\ &\times \exp \left[ -\frac{\Gamma_{at}}{4\Omega_1} [\sin(2\Omega_1 t) - \sin(2\Omega_1 t')] \right], \\ g_s^K(t, t') &= \Theta(t - t') \exp \left[ -\left( \Gamma_{s0} + \frac{\Gamma_s}{2} \right) (t - t') \right] \\ &\times \exp \left[ -\frac{2\sqrt{\Gamma_{s0}\Gamma_s}}{\Omega_1} [\sin(\Omega_1 t) - \sin(\Omega_1 t')] \right] \\ &\times \exp \left[ -\frac{\Gamma_s}{4\Omega_1} [\sin(2\Omega_1 t) - \sin(2\Omega_1 t')] \right]. \quad (35) \end{aligned}$$

We then have

$$\begin{aligned} G_{ba}^K(t, t') &= H \int_{-\infty}^{\infty} dt_1 g_s^K(t, t_1) [G_{aa}^K(t_1, t') + \Lambda_s(t_1, t')], \\ \int_{-\infty}^{\infty} dt_1 [g_{at}^K(t, t_1)]^{-1} + H^2 g_s^K(t, t_1) G_{aa}^K(t_1, t') &= \Lambda_{at}(t, t'). \quad (36) \end{aligned}$$

We realize that the non-interacting Green's functions  $g_{at/s}^{A/K}(t, t')$  oscillate on time with the frequency  $\Omega_1 = \Omega/p$ . We cannot apply any cut-off for the boundary of the integrals in the equations (28) and (36). It means we cannot solve these equations exactly. However,  $g_{at/s}^{A/K}(t, t')$  can be considered oscillating around smooth averaging functions  $\overline{g_{at/s}^{A/K}(\tau, T)}$  with  $T \gg \Omega_1^{-1}$ . It is discussed in detail in the following subsection.

### C. The Averages:

In order to find the Majorana Green's functions  $G_{aa}^A(t, t')$  and  $G_{ba}^K(t, t')$ , one needs to solve equations (28) and (36). In this subsection, we represent our averaging approximation method.

#### 1. Advanced Green's function $\overline{G_{aa}^A(\omega)}$ :

The  $g_{at/s}^A(t, t')$  in equations (27) can be expressed as functions of the Bessel function products, for instance,

$$\begin{aligned} g_{at}^A(t, t') &= -\Theta(t' - t) \sum_{m, n=-\infty}^{\infty} J_n \left( -i \frac{\Gamma_{at}}{4\Omega_1} \right) J_m \left( -i \frac{\Gamma_{at}}{4\Omega_1} \right) \\ &\times e^{\frac{\Gamma_{at}}{2}(t-t')} e^{i2\Omega_1(nt - mt')}. \quad (37) \end{aligned}$$

We change time variables such as  $\tau = t - t'$ ,  $T = (t + t')/2$ . Because the Green's functions  $g_{at/s}^A(\tau, T)$  oscillate on time with period  $2\pi\Omega_1^{-1}$ , we average them over time  $T$  in a period of  $2\pi/\Omega_1$ . We then write it in Fourier space as

$$\overline{g_{at}^A(\omega)} = \sum_{n=-\infty}^{\infty} J_n^2 \left( -i \frac{\Gamma_{at}}{4\Omega_1} \right) \frac{i}{\omega + 2n\Omega_1 - i \frac{\Gamma_{at}}{2}}. \quad (38)$$

Similarly,

$$\begin{aligned} \overline{g_s^A(\omega)} &= \sum_{m, n, k=-\infty}^{\infty} J_{m-2n+2k} \left( -i \frac{2\sqrt{\Gamma_{s0}\Gamma_s}}{\Omega_1} \right) \\ &\times J_m \left( -i \frac{2\sqrt{\Gamma_{s0}\Gamma_s}}{\Omega_1} \right) J_n \left( -i \frac{\Gamma_s}{4\Omega_1} \right) J_k \left( -i \frac{\Gamma_s}{4\Omega_1} \right) \\ &\times \frac{i}{\omega + (m+2k)\Omega_1 - i \left( \Gamma_{s0} + \frac{\Gamma_s}{2} \right)}. \quad (39) \end{aligned}$$

We thus have

$$\overline{G_{aa}^A(\omega)} = \frac{-i}{\overline{g_{at}^A(\omega)}^{-1} + H^2 \overline{g_s^A(\omega)}}. \quad (40)$$

## 2. Keldysh Green's function $\overline{G_{ba}^K(\omega)}$ :

In the same technique, we obtain the average non-interacting Green's functions

$$\overline{g_{at}^K(\omega)} = \sum_{n=-\infty}^{\infty} J_n^2 \left( i \frac{\Gamma_{at}}{4\Omega_1} \right) \frac{i}{\omega + 2n\Omega_1 + i \frac{\Gamma_{at}}{2}}, \quad (41)$$

$$\begin{aligned} \overline{g_s^K(\omega)} &= \sum_{m,n,k=-\infty}^{\infty} J_{m-2n+2k} \left( i \frac{2\sqrt{\Gamma_{s0}\Gamma_s}}{\Omega_1} \right) \\ &\times J_m \left( i \frac{2\sqrt{\Gamma_{s0}\Gamma_s}}{\Omega_1} \right) J_n \left( i \frac{\Gamma_s}{4\Omega_1} \right) J_k \left( i \frac{\Gamma_s}{4\Omega_1} \right) \\ &\times \frac{i}{\omega + (m+2k)\Omega_1 + i(\Gamma_{s0} + \frac{\Gamma_s}{2})}. \end{aligned} \quad (42)$$

We also average  $\Lambda_{at/s}(t, t')$  and obtain  $\overline{\Lambda_{at/s}(\omega)}$  as

$$\begin{aligned} \overline{\Lambda_{at}(\omega)} &= G_{aa}^A(\omega) \{ \Gamma_a [f(\omega - \Omega/p) + f(\omega + \Omega/p) - 1] \\ &+ \frac{\Gamma_t}{2} \sum_n J_n^2 \left( \frac{V_{ac}}{\Omega} \right) [f(\omega - (n+1/p)\Omega + V_{dc}) \\ &+ f(\omega + (n-1/p)\Omega - V_{dc}) + f(\omega - (n-1/p)\Omega + V_{dc}) \\ &+ f(\omega + (n+1/p)\Omega - V_{dc}) - 2] \}, \end{aligned} \quad (43)$$

$$\begin{aligned} \overline{\Lambda_s(\omega)} &= g_s^A(\omega) G_{aa}^A(\omega) \{ 2\Gamma_{s0} [2f(\omega) - 1] \\ &+ \Gamma_s [f(\omega - \Omega/p) + f(\omega + \Omega/p) - 1] \}. \end{aligned} \quad (44)$$

In this limit,  $G_{ba}^K(t, t')$  only depends on  $\tau = t - t'$  and its Fourier transform is

$$\overline{G_{ba}^K(\omega)} = \frac{H \overline{g_s^K(\omega)} \left[ \overline{g_{at}^K(\omega) \Lambda_{at}(\omega)} + \overline{\Lambda_s(\omega)} \right]}{1 + H^2 \overline{g_{at}^K(\omega)} \overline{g_s^K(\omega)}}. \quad (45)$$

The meaning of our averaging method is that we have smoothed the fine oscillations of the Green's functions. It works well in the high frequency regime, namely,  $T \gg \Omega_1^{-1}$ . It offers the opportunity to compute the physical observables non-perturbatively. Our results should be close to the exact solution while the results from the perturbation calculation cannot be. Any cut-off in the perturbation calculation will induce a loosing of some contributions in the physical observables. However, our averaging method cannot be applied for the adiabatic limit. The adiabatic regime should be considered separately, maybe as in Ref. [29]. In the next section, we calculate the differential conductance and magnetic impurity susceptibility by using this averaging method.

## IV. AVERAGE PHYSICAL OBSERVABLES

In this section we will compute average differential conductance and magnetic susceptibility, and discuss the results. We notice readers that the word "average" in this paper mostly refers our averaging method.

### A. Average charge current and average differential conductance

We are first interested in calculating the time averaged charge current through the junction  $\langle I_c \rangle$  because the time averaged differential conductance  $G = d\langle I_c \rangle / dV_{dc}$  is accessible experimentally [17]. We compute it by using the Keldysh non-equilibrium Green's function technique. The current at a time  $t$  can be written in the form

$$I_c(t) = -\frac{eJ_t(t)}{4\sqrt{\pi a}} \Re \sum_k G_{fka}^K(t, t), \quad (46)$$

where we have defined the Green's function  $G_{fka}^K(t, t)$  as  $G_{fka}^K(t, t') = -i \langle T_K \{ (c_{fk}^\dagger(t) + c_{fk}(t)) \hat{a}(t') \} \rangle$ . The current is then expressed as  $I_c(t) = -(eJ_t(t)/8\pi a) \Re \int_{-\infty}^{\infty} dt_1 J_t(t_1) m_f^K(t, t_1) G_{aa}^A(t_1, t)$ . As we apply the average condition to the Green's functions, the current at a time  $t$  means "average":  $\overline{I_c(t)} \sim \overline{m_f^K(t, t_1) G_{aa}^A(t_1, t)} \sim \overline{m_f^K(t, t_1) G_{aa}^A(t_1, t)}$  then

$$\begin{aligned} \overline{I_c(t)} &= \frac{J_t(t)}{8\pi^2 a v_F} \Im \int_{-\infty}^{\infty} dt_1 J_t(t_1) \int_{-\infty}^{\infty} d\omega \sum_n J_n^2 \left( \frac{V_{ac}}{\Omega} \right) \\ &\times [f(\omega + n\Omega - V_{dc}) - f(\omega - n\Omega + V_{dc})] \\ &\times e^{-i\omega(t-t_1)} G_{aa}^A(t_1, t). \end{aligned} \quad (47)$$

One should notice that we calculate the time averaged differential conductance, we therefore can apply our average Green's function method, which has been discussed in section III. The Majorana Green's functions  $G_{aa}^A(t_1, t)$  is calculated averagely in the above section with its Fourier image is shown in equation (40). As discussed above, the current should oscillate on time with period  $2\pi\Omega^{-1}$ . It is possible to take the average of the current over time  $t$  in a period of  $2\pi p\Omega^{-1}$ . So the average current is

$$\begin{aligned} \overline{I_c} &= \frac{\Omega}{2\pi p} \int_0^{2\pi p/\Omega} dt \overline{I_c(t)} \\ &= \frac{\Gamma_t}{8\pi} \Im \int_{-\infty}^{\infty} d\omega \sum_n J_n^2 \left( \frac{V_{ac}}{\Omega} \right) \\ &\times \{ [f(\omega + (n-1/p)\Omega - V_{dc}) \\ &- f(\omega - (n+1/p)\Omega + V_{dc}) \\ &+ f(\omega + (n+1/p)\Omega - V_{dc}) \\ &- f(\omega - (n-1/p)\Omega + V_{dc})] G_{aa}^A(\omega) \}. \end{aligned} \quad (48)$$

By taking the derivative of the time averaged current in equation (48) with respect to the dc voltage, we obtain the time averaged differential conductance. The conductance and the magnetic susceptibility behaviors remain when the temperature is varied from absolute zero to a very small temperature. If the temperature is kept increasing much below the Kondo temperature, the conductance and the susceptibility behaviors are broadened

and then smeared. For convenient computation, we consider the time averaged differential conductance at the absolute zero

$$\begin{aligned} \bar{G} = & \frac{\Gamma_t}{8\pi} \Im \sum_{n=-\infty}^{\infty} J_n^2 \left( \frac{V_{ac}}{\Omega} \right) \\ & \times \left\{ \overline{G_{aa}^A(V_{dc} - (n-1/p)\Omega)} \right. \\ & + \overline{G_{aa}^A(-V_{dc} + (n+1/p)\Omega)} \\ & \overline{G_{aa}^A(V_{dc} - (n+1/p)\Omega)} \\ & \left. + \overline{G_{aa}^A(-V_{dc} + (n-1/p)\Omega)} \right\}, \end{aligned} \quad (49)$$

where the differential conductance is defined as  $G = d \left[ \frac{\Omega}{2\pi p} \int_0^{2\pi p/\Omega} I_c(t) dt \right] / dV_{dc}$ . We will discuss the behavior of the average differential conductance as a function of magnetic field and source-drain voltage.

### B. Average impurity magnetization and susceptibility

While the experimentalists are interested in measuring average differential conductance, the theorists are interested in calculating magnetic susceptibility as well because both observables provide direct information about the magnetic impurity of a SET. The local magnetic susceptibility – the response to a magnetic field coupled to the impurity spin only – is the derivative of the magnetization, which is calculated from the following formula

$$M(H) = \frac{\mu_B g_i}{4\pi} \int_{-\infty}^{\infty} d\omega G_{ba}^K(\omega). \quad (50)$$

The Majorana Green's function  $G_{ba}^K(\omega)$  is calculated averagely in the above section with its Fourier image shown in equation (45). The magnetization is understood as the ‘‘average’’ one and is expressed as

$$M(H) = \frac{(\mu_B g_i) H}{4\pi} \int_{-\infty}^{\infty} d\omega \frac{g_s^K(\omega) \left[ \overline{g_{at}^K(\omega) \Lambda_{at}(\omega)} + \overline{\Lambda_s(\omega)} \right]}{1 + H^2 \overline{g_{at}^K(\omega) g_s^K(\omega)}}. \quad (51)$$

From formula (51), when the system is applied either a constant voltage bias  $V_{sd} = V_{dc}$  or a time dependent one  $V_{sd} = V_{dc} + V_{ac} \cos(\Omega t)$  and the Kondo couplings are time independent, again, we re-obtain the results in the SH theory [10, 21].

We compute the impurity susceptibility as  $\chi(H) = \mu_B g_i \partial_H M(H)$  and discuss its behavior in the following subsection.

### C. Results and discussions

What we show below is just a sample of some plots to give a flavor of our results. In all plots, the horizontal

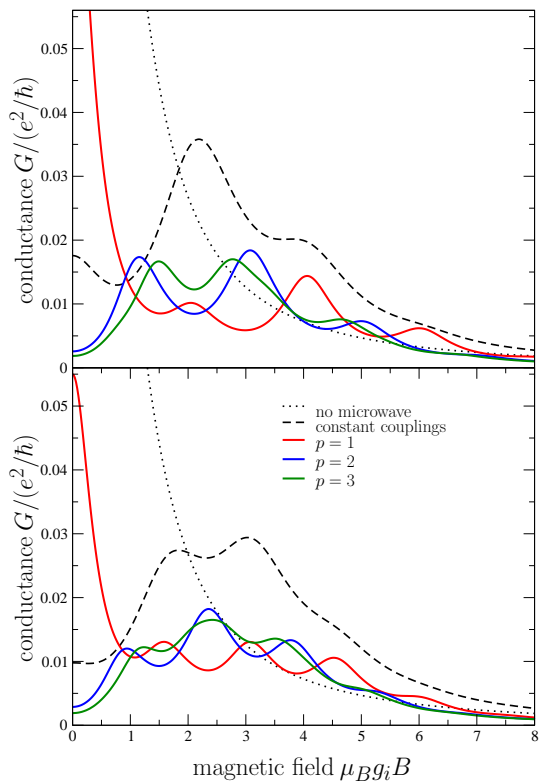


Figure 1: (Color online)  $G(H)$  are plotted for  $V_{ac} = 4$ ,  $\Gamma_{at} = 0.3$ ,  $\Gamma_s = 0.05$ ,  $\Gamma_t = 0.25$ ,  $V_{dc} = 0$ , and  $\hbar\Omega = 2$  in the upper panel and  $\hbar\Omega = 1.5$  in the lower one. The dotted black curve is without microwaves; Kondo peak at  $\mu_B g_i B = 0$ . The dashed black curve is with ac voltage, constant couplings:  $J_{\perp}^{\alpha\beta} = J_{\perp 0}^{\alpha\beta} + J_{\perp 1}^{\alpha\beta}$ ; Kondo satellites at  $\mu_B g_i B = n\hbar\Omega$ ; the highest peak's position depends on  $eV_{ac}/\hbar\Omega$ . When both voltage and couplings are oscillating, peaks occur at  $\mu_B g_i B = (n \pm 1/p)\hbar\Omega$ ; the solid red, blue, green curves are corresponding for the  $p = 1, 2, 3$ . The peak splitting due to time-dependent couplings can be seen clearly at the highest peak.

axis is the magnetic energy  $H = \mu_B g_i B$ ,  $B$  is the amplitude of applied magnetic field, the vertical axis is conductance  $G/(e^2/h)$  or magnetic susceptibility  $\chi/(g_i \mu_B)^2$ . We choose  $\Gamma_{s0} = 1$  as the energy scale and it can be considered Kondo temperature. It means the other parameter values are chosen in comparing with  $\Gamma_{s0}$ . The results obtained at very small temperature and at absolute zero are similar. For efficient numerical calculation we choose to work with conductance at absolute zero and susceptibility at very small temperature ( $T = 0.05$ ).

In figures 1 and 3, conductance  $G$  and susceptibility  $\chi$  are plotted as functions of magnetic field  $H$  for different situations: no microwave (dotted black curves), time dependent voltage (dashed black curves), and both time dependent voltage and couplings with different values of  $p$  (red curves for  $p = 1$ , blue curves for  $p = 2$ , and green curves for  $p = 3$ ). When we compare the conductance with and without the effect of microwaves, we find that



microwave irradiation reduces strongly the conductance. Because we consider a SET in a special situation of couplings, we cannot compare our results with the case where we only consider oscillation in voltage  $V_{ac}(t)$ , no time oscillation applied on couplings as we discussed in section II (no current in this situation in equilibrium). However, we can compare our result with the case in which we only consider oscillation in voltage  $V_{ac}(t)$  and constant couplings such as  $J_{\perp}^{\alpha\beta} = J_{\perp 0}^{\alpha\beta} + J_{\perp 1}^{\alpha\beta}$  so  $J_t, J_{s0} + J_s, J_a$ . The side-band effect of microwaves with the peaks appearing at  $\mu_B g_i B = eV_{dc} \pm n\hbar\Omega$  ( $n \in \mathbb{Z}$ ) due to the oscillation of source-drain voltage  $V_{ac}(t)$  [8, 10–16]. As it is mentioned in Ref. [16] the photon-induced satellites appear quite delicate, we deeply investigate the effect of ratio  $eV_{ac}/\hbar\Omega$ . The side-band peaks only appear when  $eV_{ac}/\hbar\Omega$  is big enough compare to 1 (but  $eV_{ac} \sim \hbar\Omega$ , as well as  $\hbar\Omega \sim k_B T_K$  and  $\hbar\Omega > k_B T_K$  in order to avoid decoherence), and this ratio determines the height of side-band peaks. For instance, in the upper panel of figure 1 plotted for  $1 < eV_{ac}/\hbar\Omega \leq 2$ , we see the highest peak at  $\mu_B g_i B = \hbar\Omega$  besides the trivial main peak at  $\mu_B g_i B = 0$ . The strength of microwaves is small compared to the strength of the magnetic field, which reduces strongly Kondo conductance. When we increase the oscillation amplitude, microwave effect becomes stronger than the effect of the magnetic field, it reduces strongly the peak at  $\mu_B g_i B = 0$  and increases the satellite peak at  $\mu_B g_i B = 2\hbar\Omega$  as we see in the lower panel for  $eV_{ac}/\hbar\Omega > 2$ . One can say the highest satellite peak position depends on the ratio  $eV_{ac}/\hbar\Omega$ . However, it is impossible to see the highest satellite peak at  $\mu_B g_i B = 3\hbar\Omega$  due to the strong suppression by both magnetic field and voltage. This result suggests to experimentalists an efficient method to calibrate the oscillation voltage amplitude  $V_{ac}$ .

We now discuss the second effect of microwaves. In fact, the oscillation of Kondo couplings comes from the oscillation of source-drain and gate voltages. It can be considered as an indirect effect. In figure 1 the dashed black curve is plotted for the constant couplings, the red, blue, and green curves are plotted for the time dependent couplings with  $p = 1, 2, 3$  correspondingly. We find that when the coupling parameters oscillate with frequency  $\Omega_1 = \Omega/p$  with  $p \in \mathbb{N}$ , each main peak splits into two peaks. Since the energy is conserved, when a peak is split into two peaks, the height of these two peaks relate to the height of original peak. The distance between an original peak and its split peak is  $d_{peak} = \hbar\Omega/p$ . This is understood mathematically by investigating the Green's function  $G_{aa}^A(\omega)$ . The difference between the coupling frequency and the applied frequency is described by an integer number  $p \geq 1$ . However,  $p$  cannot be too big because the slow oscillation in couplings can be considered as constant compared to the fast oscillation of voltage. When  $p = 1$ , the couplings oscillate on time with the same frequency as microwaves, the satellite peaks split

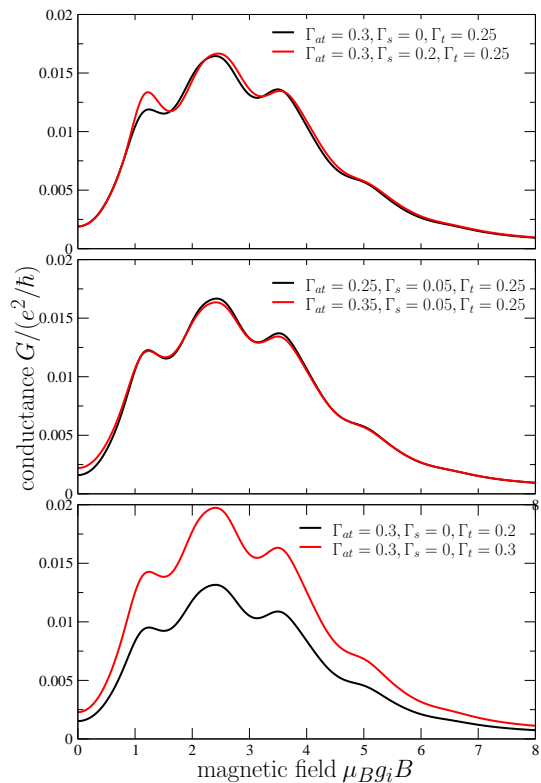


Figure 2: (Color online)  $G(H)$  are plotted for  $V_{ac} = 4$ ,  $\hbar\Omega = 1.5$ ,  $p = 3$ ,  $V_{dc} = 0$ , and different set of energy scales  $\Gamma_i$ . In the top panel,  $\Gamma_{at} = 0.3$ ,  $\Gamma_t = 0.25$  is fixed,  $\Gamma_s$  is varied:  $\Gamma_s = 0$  for the black curve,  $\Gamma_s = 0.2$  for the red curve. In the middle panel,  $\Gamma_s = 0.05$ ,  $\Gamma_t = 0.25$  is fixed,  $\Gamma_{at}$  is varied:  $\Gamma_{at} = 0.25$  for the black curve,  $\Gamma_{at} = 0.35$  for the red curve. In the bottom panel,  $\Gamma_{at} = 0.3$ ,  $\Gamma_s = 0$  is fixed,  $\Gamma_t$  is varied:  $\Gamma_t = 0.2$  for the black curve,  $\Gamma_t = 0.3$  for the red curve. Notice conductance amplitude strongly depends on  $\Gamma_t$ .

into two peaks with the distance  $d_{peak} = \hbar\Omega$  equal to the satellite peak distance. So for  $p = 1$ , the peaks remain but their height changes drastically due to the re-contribution of energy through the peak splitting. This peak splitting effect can be seen clearly if  $p = 2$ , or  $p = 3$ . As we have explained the number  $p$  can also be bigger than 1 due to the delay of phase between the source-drain voltage and gate voltage. The peak splitting can be seen clearly at the highest satellite peak. When we increase  $p$  the splitting distance  $d_{peak}$  decreases, the splitting becomes weak then approaches the limit in which the couplings are constant. This result explains well a possibility in experimental result in which one sees peaks appearing at a distance  $\mu_B g_i B < \hbar\Omega$  in the regime of weak magnetic field. We predict  $p$  is a frequency dependent systematic parameter. It should be checked carefully in experimentation. For the case  $p = 1$ , we can check the height of the satellite peaks to confirm the two fold effect of microwave on voltage and couplings.

Besides, from figure 2, we find the main characteristic of  $G(H)$  lightly depends on scales  $\Gamma_i$ , ( $i = at, s, t$ ).

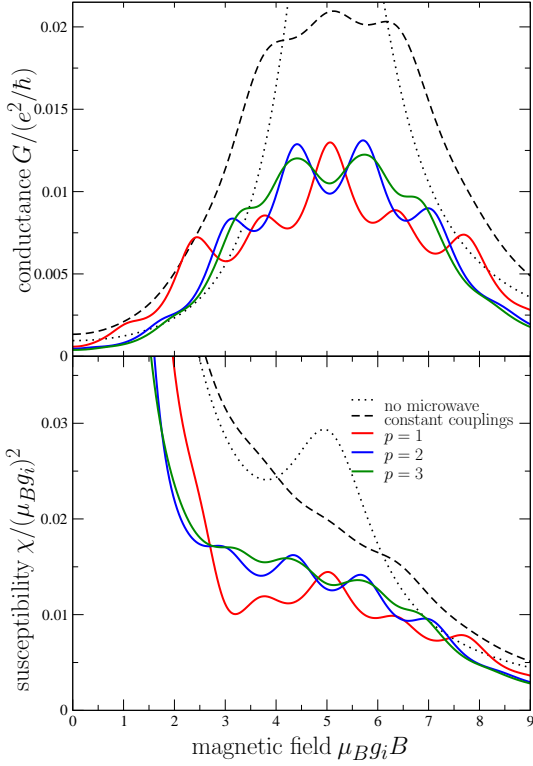


Figure 3: (Color online)  $G(H)$  and  $\chi(H)$  are plotted in the upper and lower panels correspondingly for  $\hbar\Omega = 1.35$ ,  $eV_{ac} = 2$ ,  $V_{dc} = 5$ ,  $\Gamma_{at} = 0.3$ ,  $\Gamma_s = 0.1$ ,  $\Gamma_t = 0.25$ . The dotted black curve is without microwaves; Kondo peak at  $\mu_B g_i B = eV_{dc}$ . The dashed black curve is with ac voltage, constant couplings:  $J_{\perp}^{\alpha\beta} = J_{\perp 0}^{\alpha\beta} + J_{\perp 1}^{\alpha\beta}$ ; Kondo satellites at  $\mu_B g_i B = eV_{dc} \pm n\hbar\Omega$ . When both voltage and couplings are oscillating, peaks occur at  $\mu_B g_i B = eV_{dc} \pm (n \pm 1/p)\hbar\Omega$ ; the solid red, blue, green curves are corresponding for the  $p = 1, 2, 3$ .

$\Gamma_i$  are chosen much smaller than  $\Gamma_{s0}$  because the microwave effects on the couplings should be small compared to the existing couplings. We vary each energy scale  $\Gamma_s$ ,  $\Gamma_{at}$ ,  $\Gamma_t$  in the top, middle, and bottom panel correspondingly while other parameters are fixed.  $\Gamma_t \sim (J_{\perp}^{LR})^2$  concerns the coupling between two leads and it controls the spin-flip tunneling of electrons through QD.  $\Gamma_s \sim [J_{\perp}^{LL} + J_{\perp}^{RR}]^2$  concerns the sum of separated couplings in each lead and is small compared to  $\Gamma_{s0}$ .  $(J_{\perp}^{LL} - J_{\perp}^{RR})^2$  contributes to  $\Gamma_{at}$ . Both energy scales  $\Gamma_{at}$  and  $\Gamma_s$  affect slightly the  $G(H)$  behavior. The red curve in the bottom panel is plotted for the case in which modulation of microwave only affects the transverse couplings, so  $\Gamma_{at} = 0.3$ ,  $\Gamma_s = 0$ ,  $\Gamma_t = 0.3$ . The amplitude of conductance strongly decreases when we decrease  $\Gamma_t$ . It vanishes when  $\Gamma_t = 0$ . Thus, any small effect of microwave irradiation drives the system away from the uncoupled isotropic two-channel Kondo situation.

In figure 3, the magnetic susceptibility is plotted as a function of magnetic field at temperature  $T = 0.05$ . As previously stated from  $G(H)$  characteristic, dc voltage

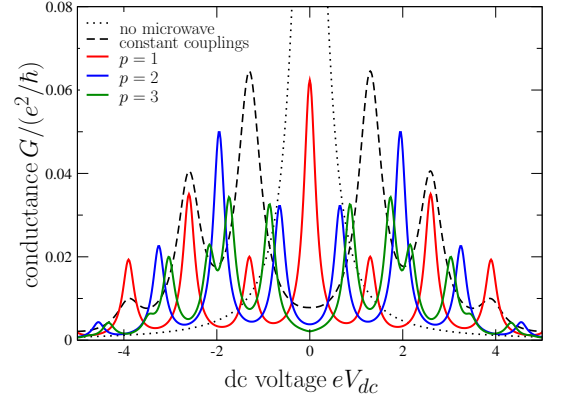


Figure 4: (Color online)  $G(V_{dc})$  is plotted for  $\hbar\Omega = 1.3$ ,  $eV_{ac} = 3$ ,  $\Gamma_{at} = 0.3$ ,  $\Gamma_s = 0.05$ ,  $\Gamma_t = 0.2$ ,  $H = 0$ . The dotted black curve is without microwaves; Kondo peak at  $eV_{dc} = 0$ . The dashed black curve is with ac voltage, constant couplings; Kondo satellites at  $eV_{dc} = \pm n\hbar\Omega$ . When both voltage and couplings are oscillating, peaks occur at  $eV_{dc} = \pm (n \pm 1/p)\hbar\Omega$ ; the solid red, blue, green curves are corresponding for the  $p = 1, 2, 3$ .

$V_{dc}$  also splits the satellite peaks [8] when it is smaller than the ac voltage  $V_{ac}$ . It may cause confusion to recognize the peak splitting due to the oscillations of couplings in experiment if experimentalists cannot avoid a small contribution of  $V_{dc}$ . The fact that  $V_{dc}$  splits peaks by a distance  $\pm eV_{dc}$  is understood in non-equilibrium Kondo physics of a QD without microwave irradiation [21]. Significantly, if  $V_{dc}$  is bigger than  $V_{ac}$ , we see the peak splitting due to the oscillations of couplings. If  $V_{dc} = 0$ , we see the satellite peaks dominate at  $\mu_B g_i B = 0$ . The other peaks at  $\mu_B g_i B = k\hbar\Omega$  ( $k = \pm 1, \pm 2, \dots$ ) are very weak. To study the satellite peak splitting due to coupling oscillation, we choose  $V_{dc} > V_{ac}$ . We find all susceptibility-magnetic field and conductance-magnetic field characteristics are the same. It is evident that the relation between susceptibility and conductance shown in formula (8.9) of Ref. [21] can be generalized when the system is irradiated by microwaves.

The differential conductance  $G$  and magnetic susceptibility  $\chi$  are also plotted as functions of dc voltage  $V_{dc}$  in figures 4 and 5. In order to investigate microwave irradiation effect, we consider the case in which no magnetic field is applied. Again, we find the two-fold peak splitting (Kondo satellite splitting) due to both voltage and Kondo coupling oscillations. There is more challenge for experimentalists if we are in the cases  $p = 1$  and  $p = 2$ . The distance between peaks is still  $\hbar\Omega$ . For  $p = 1$ , the positions of peaks are the same as those in the case when only voltage oscillates, but the peak heights are re-contributed. For  $p = 2$ , both the positions and heights of peaks are re-contributed, satellite peaks are shifted by  $\hbar\Omega/2$ . For  $p \geq 3$ , our interesting results show that one has a chance to see two peaks, whose distance is much smaller than  $\hbar\Omega$ . For instance, in the green curves

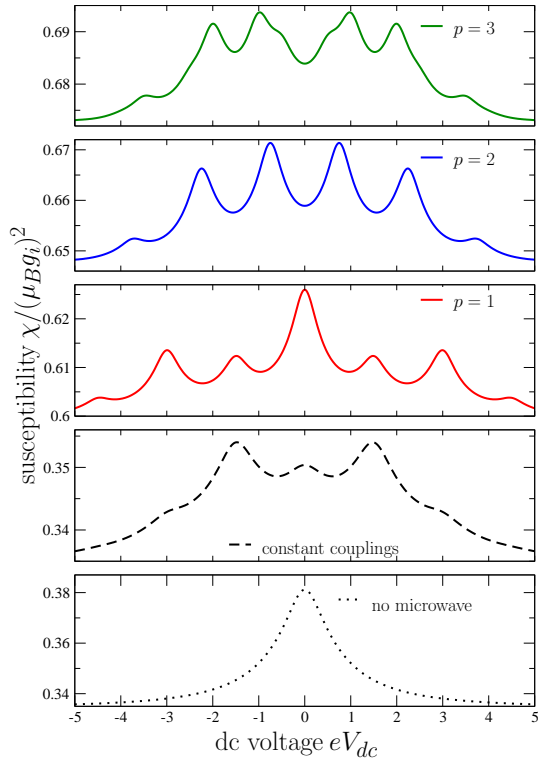


Figure 5: (Color online)  $\chi(V_{dc})$  is plotted for  $\hbar\Omega = 1.5$ ,  $eV_{ac} = 2.5$ ,  $\Gamma_{at} = 0.3$ ,  $\Gamma_s = 0.1$ ,  $\Gamma_t = 0.25$ ,  $H = 0$ . The dotted black curve is without microwaves; Kondo peak at  $eV_{dc} = 0$ . The dashed black curve is with ac voltage, constant couplings; Kondo satellites at  $eV_{dc} = \pm n\hbar\Omega$ . When both voltage and couplings are oscillating, peaks occur at  $eV_{dc} = \pm(n \pm 1/p)\hbar\Omega$ ; the solid red, blue, green curves are corresponding for the  $p = 1, 2, 3$ .

in figures 4 and 5, which are plotted for  $p = 3$ , one can find two peaks which are split from a satellite peak at a distance of  $2\hbar\Omega/3$ . Moreover, one can also find two peaks at a distance of  $\hbar\Omega/3$ . They are the peaks, that are split from the consecutive satellite peaks.

## V. CONCLUSIONS

In this paper, we have investigated the effect of microwave irradiation on a SET in a magnetic field. The frequency of the microwaves is  $\Omega$ . The system is described by a non-equilibrium Kondo model in a specific point in the parameter space, where the Hamiltonian  $\mathcal{H}$  can be diagonalized. Besides the oscillation in the source-drain voltage, the oscillation in the Kondo couplings is investigated for a specific situation. The Kondo couplings  $J_{\perp}^{\alpha\beta}(t)$  relate to the source-drain voltage and the gate voltage, which oscillate with frequency  $\Omega$ . The couplings thus oscillate on time with the same frequency or its harmonics. However, one can think about an appropriate experimental set-up, in which the Kondo couplings  $J_{\perp}^{\alpha\beta}(t)$

oscillate with a frequency  $\Omega_1 = \Omega/p$ ,  $p \in \mathbb{N}$ . The time dependent parts in  $J_{\perp}^{\alpha\beta}(t)$  drive the system away from the isotropic two channel Kondo problem to the anisotropic one though their amplitudes are small compared to the time independent parts. Due to the oscillations in the input parameters, the interacting Green's functions oscillate on time with a frequency of  $\hbar\Omega/p$ ; thus the problem cannot be solved exactly. However, these fast oscillations allow one to average Green's functions and observables in a period  $2\pi p/\Omega$ . We have proposed a non-perturbative approximation, in which we have smoothed the fine fast oscillations around its average form. Thus, the Green's functions and the observables are averaged. Our averaging method gives the results, which are closed to the exact one. The higher the frequency, the better the approximation result. It works well for the cases  $\hbar\Omega \gtrsim k_B T_K \sim \Gamma_{s0} \gg \Gamma_{at/s/t}$  in which we study Kondo satellite peaks.

The center result of our work is the satellite peak splitting. This feature happens when oscillation parts are added to the Kondo couplings in a particular situation. The distance between two peaks, which are split from a satellite, is  $2\hbar\Omega/p$ , the distance between two peaks, which are split from two consecutive satellites, is  $(p-1)\hbar\Omega/p$ , while the distance between two satellites is  $\hbar\Omega$ . All the new distances in our results depend on the number  $p$ , which describes the difference between the frequency of the Kondo couplings and the frequency of input microwaves. We see the two close peaks clearly at small magnetic field in  $G(H)$ ,  $\chi(H)$  characteristics and small dc voltage in  $G(V_{dc})$ ,  $\chi(V_{dc})$  characteristics.

Magnetic field and applied dc and ac voltages suppress the Kondo correlation alternatively. When a dc source-drain voltage  $V_{dc}$  is applied, the equilibrium Kondo peak is split into two peaks [6, 7]. The distance from the original peak to one of the new ones is  $d_{peak} = eV_{dc}$ . When a magnetic field  $B$  is applied, the Kondo peak is also split into two peaks with  $d_{peak} = \mu_B g_i B$  [6, 30]. When an ac source-drain voltage is applied, the Kondo peak is expanded into satellites with  $d_{peak} = n\hbar\Omega$  [8, 10–14]. When all above external fields are applied to a SET, the equilibrium Kondo peak is split into satellites. The position of a satellite is  $\pm eV_{dc} \pm \mu_B g_i B \pm (n \pm 1/p)\hbar\Omega$  when the Kondo couplings are considered oscillating on time with frequency  $\hbar\Omega/p$ .

Although some works, in which the time dependent exchange interactions like Kondo couplings  $J(t)$  were considered, have been done by solving flow equations [31], the exact solution for time dependent Kondo model still remains. In our work, we proposed the averaging method, which is good for high frequency regime. We predict that another method is needed for the adiabatic regime. Besides, one can discuss more carefully about the effect of microwave irradiation on the Kondo channels. Moreover, our work suggests qualitatively experimentalists set up experiments in which more than one frequency is acti-

vated [17].

## VI. ACKNOWLEDGMENTS

We gratefully acknowledge Carlos Bolech and Nayana Shah for the project suggestion and numerous discussions. The discussions with Andrei Kogan and Bryan Hemingway on experimental realization and their data sharing are gratefully acknowledged. We are thankful to Tran Minh Tien for a fruitful discussion about integral equations and to Philippe Dollfus for their review. This work is supported by University of Cincinnati.

- 
- [1] J. Kondo, Prog. Theor. Phys. Osaka **32**, 37 (1964).  
 [2] A.C. Hewson, *The Kondo Problem to Heavy Fermions, Cambridge Studies in Magnetism* (Cambridge University Press, Cambridge, U.K., 1993).  
 [3] L.I. Glazman and M.E. Raikh, Pis'ma Zh. Eksp. Teor. Fiz. **47**, 378 (1988) [JETP Lett. **47**, 453 (1988)]; T.K. Ng and P.A. Lee, Phys. Rev. Lett. **61**, 1768 (1988); S. Hershfield, J.H. Davies, and J.W. Wilkins, Phys. Rev. Lett. **67**, 3720 (1991).  
 [4] D. Goldhaber-Gordon, H. Shtrikman, D. Mahalu, D. Abusch-Magder, U. Meirav, and M.A. Kastner, Nature (London) **391**, 156 (1998); S. M. Cronenwett, T. H. Oosterkamp, and L. P. Kouwenhoven, Science **281**, 540 (1998); J. Schmid, J. Weis, K. Eberl, and K. von Klitzing, Physica B **256–258**, 182 (1998).  
 [5] for a review, see M. Pustilnik, L. Glazman, Journal of Physics Condensed Matter **16**, R513 (2004).  
 [6] Y. Meir, N.S. Wingreen, and P.A. Lee, Phys. Rev. Lett. **70**, 2601 (1993).  
 [7] T. K. Ng, Phys. Rev. Lett. **70**, 3635 (1993); M.H. Hettler, J. Kroha, and S. Hershfield, Phys. Rev. Lett. **73**, 1967 (1994).  
 [8] M.H. Hettler and H. Schoeller, Phys. Rev. Lett. **74**, 4907 (1995).  
 [9] T.K. Ng, Phys. Rev. Lett. **76**, 487 (1996).  
 [10] A. Schiller and S. Hershfield, Phys. Rev. Lett. **77**, 1821 (1996).  
 [11] Y. Goldin and Y. Avishai, Phys. Rev. Lett. **81**, 5394 (1998); Phys. Rev. B **61**, 16750 (2000).  
 [12] R. López, R. Aguado, G. Platero, and C. Tejedor, Phys. Rev. Lett. **81**, 4688 (1998); Phys. Rev. B **64**, 075319 (2001).  
 [13] A. Kaminski, Yu.V. Nazarov, and L.I. Glazman, Phys. Rev. Lett. **83**, 384 (1999); Phys. Rev. B **62**, 8154 (2000).  
 [14] P. Nordlander, N.S. Wingreen, Y. Meir, and D.C. Langreth, Phys. Rev. B **61**, 2146 (2000).  
 [15] P.K. Tien and J.P. Gordon, Phys. Rev. **129**, 647 (1963).  
 [16] A. Kogan, S. Amasha, M.A. Kastner, Science **304**, 1293 (2004).  
 [17] B. Hemingway, A. Kogan, private communication.  
 [18] V.J. Emery and S. Kivelson, Phys. Rev. B **46**, 10 812 (1992).  
 [19] the different experimental set-ups for different scenarios of microwave effects have been discussed with Andrei Kogan's group.  
 [20] J. Appelbaum, Phys. Rev. Lett. **17**, 91 (1966); P.W. Anderson, Phys. Rev. Lett. **17**, 95 (1966).  
 [21] A. Schiller and S. Hershfield, Phys. Rev. B **58**, 14978 (1998).  
 [22] K. Le Hur and G. Seelig, Phys. Rev. B **65**, 165338 (2002); T.K.T. Nguyen, M.N. Kiselev, and V.E. Kravtsov, Phys. Rev. B **82**, 113306 (2010).  
 [23] The detailed bosonization technique can be found in text books and review articles, for instance, T. Giamarchi, *Quantum Physics in One Dimension*, (Oxford University Press, New York, 2004).  
 [24] The Keldysh Green's function technique can be found in several text books as well as review articles, we show here one book, in which we follow the detail technique: A.M. Zagoskin, *Quantum Theory of Many-Body Systems: Techniques and Applications*, in series *Graduate Texts in Contemporary Physics*, (Springer-verlag, Berlin and Heidelberg, 1998).  
 [25] A.-P. Jauho, N.S. Wingreen, and Y. Meir, Phys. Rev. B **50**, 5528 (1994).  
 [26] M. Heyl and S. Kehrein, Phys. Rev. B **81**, 144301 (2010).  
 [27] O. A. Tretiakov and A. Mitra, Phys. Rev. B **81**, 024416 (2010).  
 [28] M.T. Tran, Phys. Rev. B **78**, 125103 (2008).  
 [29] A. Schiller and A. Silva, Phys. Rev. B **77**, 045330 (2008).  
 [30] A. Kogan, S. Amasha, D. Goldhaber-Gordon, G. Granger, M.A. Kastner, and H. Shtrikman-Shtrikman, Phys. Rev. Lett. **93**, 166602 (2004).  
 [31] D. Lobaskin and S. Kehrein, Phys. Rev. B **71**, 193303 (2005); P. Wang, S. Kehrein, Phys. Rev. B **82**, 125124 (2010); C. Tomaras and S. Kehrein, EPL **93** 47011 (2011).